Investigating Fueling Location and Transient Fueling Effects on SOL Transport in MAST-U

Y. Damizia[1,2], S. Mordijck[1], N. Walkden[2], J. Lovell[3], S. Thomas[4],

and the MAST-U Team*
[1]William & Mary, Williamsburg, VA, USA
[2]UKAEA (United Kingdom Atomic Energy Authority), Culham Campus, Abingdon, Oxfordshire, OX14 3DB, UK
[3]Oak Ridge National Laboratory, Oak Ridge, TN, USA
[4]MIT Plasma Science and Fusion Center, Cambridge, MA, USA

Abstract

Time-resolved Thomson scattering (TS) on three ohmic L-mode MAST-U discharges shows that a single low-field side (LFS) deuterium puff can reshape edge and scrape-off layer (SOL) transport. A 100 ms puff (shot #45325) broadens the SOL in under 70 ms and leaves a residual far-SOL electron density after the valve closes. Two shorter 50 ms puffs injected 100 ms apart ($t_{\mathrm{puff}} = 0.4s$ for shot #45324, and $t_{\mathrm{puff}} = 0.5s$ for shot #45323) demonstrate a clear two-stage response. During the injection every Thomson scattering channel in the range $(R - R_{\mathrm{sep}})_{\mathrm{OMP}} = -10$ cm to +5 cm rises on a common characteristic rise time, τ_{rise}, indicating the increase is directly linked to, and dominated by, the gas puff. Once the source is removed the electron density with early gas puff drains three-to-eight times more slowly than with the delayed puff, revealing the fall in density is dominated by transport that depends on the instantaneous edge state. Puff timing therefore provides an independent knob for regulating SOL broadening and particle retention, and the combined shoulder and time-constant study using TS data offers a framework for investigate edge-particle dynamics.

1 Introduction

Understanding particle transport and density-profile formation in the scrape-off layer (SOL) is critical for both plasma confinement and power-exhaust control. A particularly important phenomenon is the formation of a *density shoulder*, a sudden broadening or flattening of the far-SOL density gradient, which has been documented on several tokamaks, including JET, ASDEX-Upgrade (AUG) and EAST [1, 2, 3]. Detailed measurements indicate that the shoulder is preceded by a regime change in filament dynamics [4]: once divertor collisionality or recycling exceeds a threshold, filaments detach from sheath control, grow in size and speed, and drive a strongly convective cross-field particle flux that ultimately broadens the SOL and enhances main-chamber fueling. Empirically, the trigger condition is set by divertor parameters: in JET and AUG a normalised collisionality $\Lambda_{\mathrm{div}} \gtrsim 1$ marks the transition [1, 2], whereas in EAST the critical divertor neutral pressure is $\sim 10^{-2}$ Pa [3]. Beyond such thresholds the shoulder can persist, even after external fueling is reduced, hinting at a hysteresis in the edge-transport response. This contribution reports on dedicated ohmic L-mode experiments from the first MAST-U campaign (MU01).

2 Experimental Setup

Three ohmic L-mode discharges (#45323–#45325) constitute the data set analyzed in this work. All discharges were ohmically heated, single-null L-mode plasmas with plasma current $I_p = 450$ kA. The strike-point positions were held fixed by real-time magnetic feedback, ensuring that variations in SOL profiles could be attributed primarily to the fueling schemes. During the flat-top the line-averaged density remained in the range $\bar{n}_e = (1\text{–}2) \times 10^{19}\,\mathrm{m}^{-3}$, a regime where the predicted L–H *power* threshold for MAST-U exceeds the available ohmic input power; the plasmas therefore stayed safely in L-mode throughout the experiment. Each shot received a single deuterium puff from the LFS valve at a nominal

*See author list of J. R. Harrison et al., *Nucl. Fusion* **64**, 112017 (2024).

particle flux of 1.5×10^{21} #/ s^{-1}. In shots #45323 and #45324 a 50 ms pulse was applied, beginning at $t = 0.50$ s and $t = 0.40$ s, respectively, so the two injections are separated by 100 ms. Shot #45325 employed a longer 100 ms puff of the same fueling rate at $t_0 = 0.40s$; the additional fueling led to a disruption yet generated a clear density shoulder. An overview of the line-averaged electron density, tangential D_α emission, and programmed LFS valve flux for all three shots is presented in Figure 1, highlighting the distinct puff timings and the resulting plasma responses.

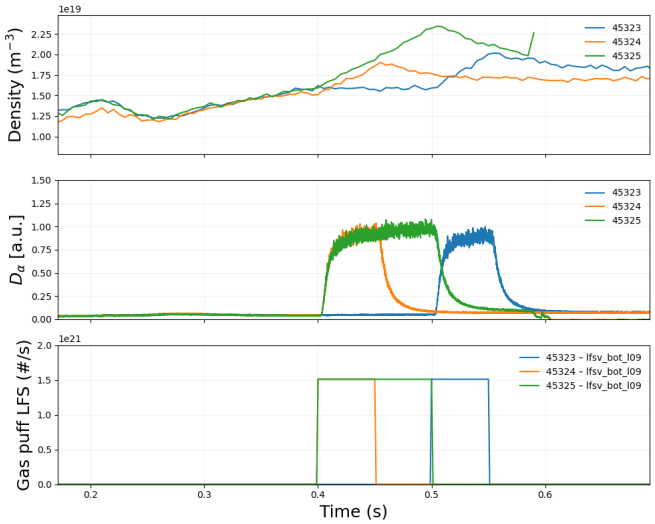

Figure 1: Discharge overview for shots #45323–#45325: (Top) line-averaged core density n_e, (Middle) tangential D_α emission, (Bottom) programmed gas-puff flux for the LFS vertical valve (lfsv_bot_l09). Each trace is color-coded by shot number.

Upstream profiles were obtained with the Thomson scattering system operated in burst mode: each measurement burst consists of eight laser shots separated by only a few microseconds, and successive bursts are triggered approximately every ∼33 ms; the eight shots in a burst are averaged to form one profile. The outermost TS channels extend 4–6 cm beyond the separatrix, capturing the far-SOL with 1 cm spatial resolution. Edge recycling was inferred from a tangential D_α filterscope. Line-integrated core densities were measured by a CO_2 interferometer, while the separatrix location was estimated using the two-point model [5], assuming a typical electron temperature at the separatrix $T_{e,sep} \approx 25$ eV for $I_p = 450$ kA, consistent with recent measurements on MAST-U [6]. These positions were used to map the Thomson scattering data in time and space. These discharges provide a direct data set to evaluate how LFS fueling modulate SOL width, shoulder formation and any memory effects. The experimental results and their interpretation will be detailed in the following sections.

3 SOL broadening and Gas-puff modulation

Figure 2 displays TS density profiles for shot 45325 at four moments spanning the 100 ms LFS gas puff. In the top graph is shown the n_e evolution and how it increases and decreases according with the gas injection. In the bottom graph, all curves are normalized to the instantaneous separatrix value $n_{e,sep}$, so each starts at $n_e/n_{e,sep} = 1$ on the $(R - R_{sep})_{OMP}$=0 axis, to focus on shape changes.

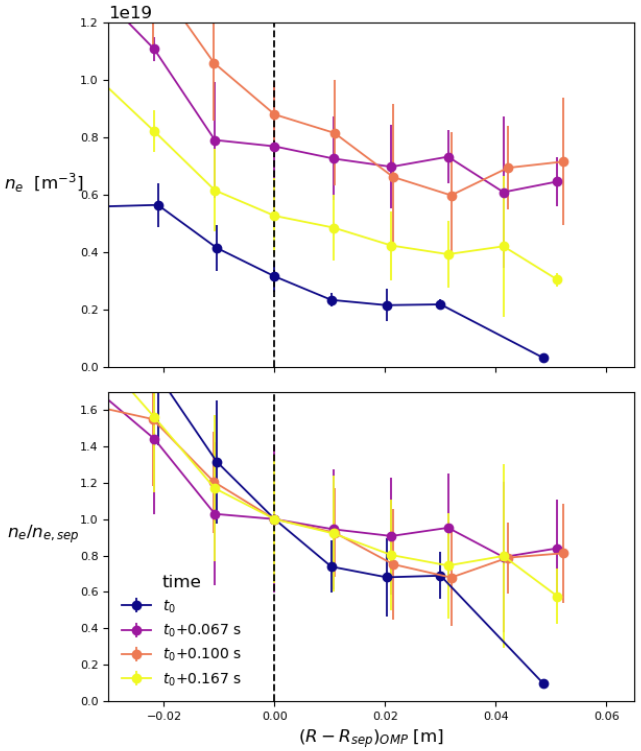

Figure 2: Electron density Thomson scattering profiles during the 100 ms LFS gas puff in discharge #45325.Top: n_e profiles. Bottom each trace is scaled by the separatrix density ($n_e/n_{e,sep}$). Legend entries mark elapsed time since the starting point of the gas puff at $t_0 = 0.40s$. Error bars are the standard deviation of the time points averaged. The sequence illustrates the transient shoulder that develops during the puff and its partial relaxation afterwards.

At $t = t_0$ (dark-blue) the profile is still steep in the SOL and shows no obvious shoulder. Early in the puff (t_0+67 ms, magenta) the density between $0.03 < (R - R_{sep})_{OMP} < 0.05$ m (far-SOL) rises, hinting at the onset of a shoulder. The flattening is clearest by the end of the puff (t_0+100 ms, salmon): the shoulder extends until $(R - R_{sep})_{OMP} \approx 0.05$ m. After the valve closes (t_0+167 ms, yellow) the absolute values of density has largely recovered and the far-SOL density is trending downwards, yet remains above the pre-puff curve at $(R - R_{sep})_{OMP} \approx 0.04$ within the error

bars. Whether this broadening is produced mainly by local ionization of the injected neutrals or by a transient enhancement of cross-field transport[7, 8] cannot be determined from the present data; both mechanisms are compatible with the observations. Nevertheless, the fact that a residual population persists in the far-SOL after the valve closes points towards a temporary change in radial transport rather than a purely source-driven effect. A definitive distinction will require additional measurements: e.g. a neutral pressure gauge, spectroscopic inversion of Balmer light to map the ionization source, or coupled SOLPS-ITER/DEGAS-2 simulations to track neutral penetration, to quantify any change in turbulent transport.

3.1 Edge response

This section compares shots 45323 and 45324 to quantify, at each radial location, the characteristic e-folding time constants that describe how the local electron density responds to the gas puff. Figure 3 illustrates an example of the fit obtained from the TS profiles at $(R - R_{\mathrm{sep}})_{\mathrm{OMP}} = -0.05$ for the two shots.

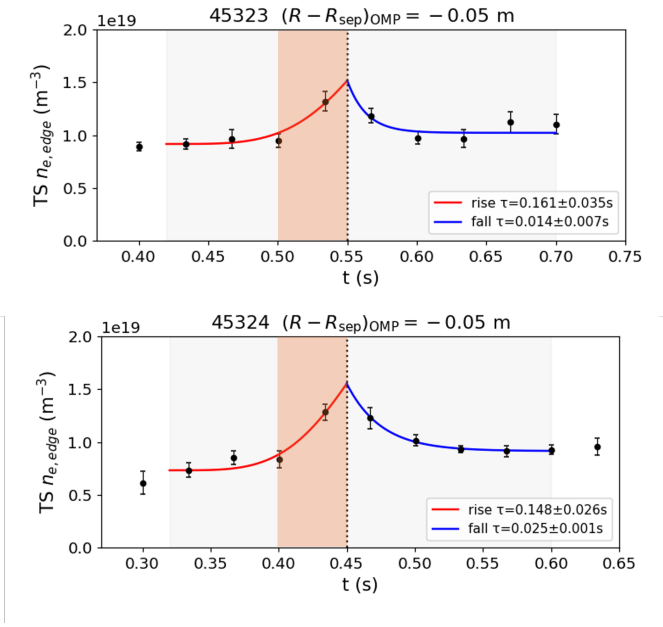

Figure 3: Example fits at $(R-R_{\mathrm{sep}})_{\mathrm{OMP}} = -0.05$ m. Red: rise, Blue: fall; the orange shaded band marks the 50 ms puff. The early puff (#45324) exhibits a longer fall time.

For every Thomson scattering channel in the range $-10\,\mathrm{cm} \le (R - R_{\mathrm{sep}})_{\mathrm{OMP}} \le +5\,\mathrm{cm}$, we model the local electron density response with a single exponential during the puff, and another after the valve closes. Let t_{on} and t_{off} denote the valve open and shut times. The density is then fitted with:

$$n_e(t) = \begin{cases} n_{e,0} + (n_{e,\mathrm{peak}} - n_{e,0})\, e^{\frac{(t-t_{\mathrm{off}})}{\tau_{\mathrm{rise}}}}, & t < t_{\mathrm{off}}, \\ n_{e,1} + (n_{e,\mathrm{peak}} - n_{e,1})\, e^{-\frac{(t-t_{\mathrm{off}})}{\tau_{\mathrm{fall}}}}, & t \ge t_{\mathrm{off}}. \end{cases} \quad (1)$$

where $n_{\mathrm{e},0}$ = density just before the puff, $n_{\mathrm{e,peak}}$ = density at the instant the valve closes, and $n_{e,1}$ = asymptotic post-puff baseline. The two free time constants, τ_{rise} and τ_{fall}, quantify how quickly the local density fills and drains, respectively.

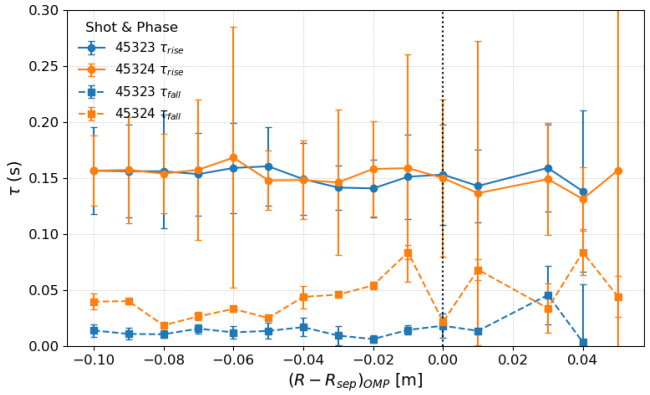

Figure 4: Local e-fold time-constants extracted from single-exponential fits to Thomson scattering density traces. Orange symbols: early puff (shot 45324, valve opened at t_0); blue symbols: delayed puff (shot 45323, valve opened at t_0+100 ms). (circles)τ_{rise}; (squares)τ_{fall}. Vertical dashed line marks the separatrix.

The e-folding time-constants τ_{rise} and τ_{fall} are obtained by data analysis fitting the TS data. Figure 4 shows a nearly flat $\tau_{\mathrm{rise}} \simeq 0.15$ s (circle) across the edge and SOL for *both* discharges indicating no difference during the puff. Instead the τ_{fall} (square) of shot #45324 climb while #45323 remains flat: between $(R - R_{\mathrm{sep}})_{\mathrm{OMP}} = -0.05$ m and the separatrix the early-puff τ_{fall} rises from ~ 0.03 s to 0.06 s, whereas the delayed-puff values stay near 0.01–0.02 s suggesting a change in the edge dynamics. The blue circles in Figure 5 shows the shot-to-shot ratio $R_{\mathrm{rise}} = \tau_{\mathrm{rise}}^{45324}/\tau_{\mathrm{rise}}^{45323}$, which clusters around unity, confirming that a 100 ms timing shift has no discernible impact on how quickly the puffed neutrals ionize and fill the edge. The red squares shows the ratio $R_{\mathrm{fall}} = \tau_{\mathrm{fall}}^{45324}/\tau_{\mathrm{fall}}^{45323}$. The R_{fall} value for $(R - R_{\mathrm{sep}})_{\mathrm{OMP}} < 0$, fluctuate around 2, but just near the separatrix the early puff (#45324) relaxes far more slowly $\tau_{\mathrm{fall}} = 0.05$–$0.09$ s versus 0.02–0.03 s for #45323, so the time-constant ratio rises to 3–8 indicating that an earlier puff leaves a weakly coupled shoulder whereas a 100 ms delay flushes the SOL rapidly. This analysis suggest that during the gas injection, edge response is governed by direct ionization; once the valve closes, the decay is instead

transport dominated.

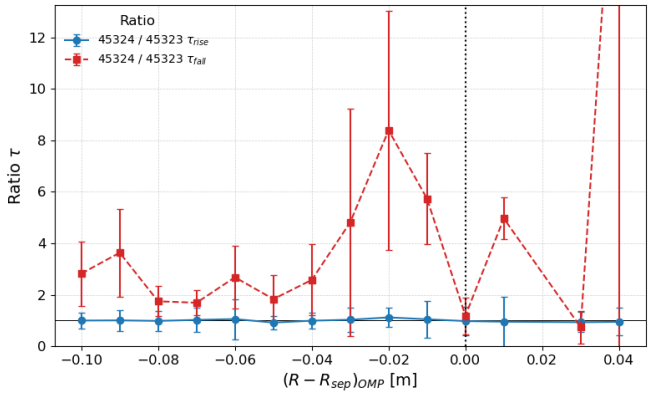

Figure 5: Shot-to-shot ratio of the time-constants in Figure 4, $\tau_{45324}/\tau_{45323}$, plotted over the same $(R - R_{\text{sep}})_{\text{OMP}}$ range. (blue circles) Rise phase; (red squares) Decay phase. Values > 1 indicate that the early puff (45324) responds more slowly at that location, values < 1 the opposite. Error bars propagate the uncertainties of the individual fits.

4 Conclusions

A single 100 ms low–field side gas puff in shot #45325 produced a shoulder broadening evolution. Before the puff the profile remained steep outside the separatrix and showed no shoulder. By t_0+67 ms the density at $0.03 < (R - R_{\text{sep}})_{\text{OMP}} < 0.05$ m had already risen, signaling the onset of a shoulder. At the end of the puff (t_0+100 ms) the flattened region extended out to $(R - R_{\text{sep}})_{\text{OMP}} \simeq 0.05$ m and the far-SOL gradient was almost erased. After the valve closed the gradient recovered within ∼70 ms, yet a residual population persisted: the density at $(R - R_{\text{sep}})_{\text{OMP}} \approx 0.04$ m remained measurably above its pre-puff value, indicating that the puff leaves a short-lived particle in the far SOL. The diagnostics available cannot yet determine whether this persistence is driven by local ionization of injected neutrals or by a transient enhancement of cross-field transport; nevertheless, the experiment shows that LFS fueling can widen the edge-density footprint in ohmic L-mode MAST-U plasmas. This result provides a quantitative baseline for future comparisons with alternative fueling geometries and for assessing the timescales over which the edge relaxes once the external source is removed. In the comparison between two shots, the edge reacts to the LFS pulse in two clearly separated stages. During the 50 ms injection in shots #45324 (early pulse, valve at $t_0 = 0.40s$) and #45323 (delayed pulse, valve at t_0+100 ms) the density in every channel from $(R - R_{\text{sep}})_{\text{OMP}} = -10$ cm to +5 cm rises on the same $\tau_{\text{rise}} \simeq 150$ ms, showing that build-up is set by neutral ionization and is indifferent to a 100 ms timing shift. After the valve closes the behavior changes, in the edge and the near-SOL, the early puff (#45324) drains three-to-eight times more slowly than the delayed puff (#45323), revealing that the exhaust is now transport-limited and sensitive to the moment at which the plasma is fueled. These results suggests that SOL width and edge-density evolution depend not only on neutral flux and injection geometry but also on the instantaneous edge state at the moment of fueling. Analyzing the shoulder broadening (shot #45325) and time-costant τ (shots #45323–#45324), yields a qualitative framework for diagnosing edge-particle retention and exhaust dynamics. Future work will extend this methodology to systematic scans of edge temperature, injections from high-field side and private flux region valves, and coupled neutral–plasma simulations aimed at refining reactor-relevant fueling strategies.

Acknowledgements

Work supported by DOE Awards DE-SC0023289, DE-SC0023372 and DE-AC05-00OR22725, and by the Engineering and Physics Sciences Research Council [grant number EP/W006839/1].

References

[1] A. Wynn *et al.*, "Scrape-off layer density shoulder formation and evolution in JET," *Nucl. Fusion*, vol. 58, 066001, 2018. doi:10.1088/1741-4326/aab4b4.

[2] L. Carralero *et al.*, "Density shoulder formation in ASDEX Upgrade L-mode plasmas," *Nucl. Fusion*, vol. 57, 056044, 2017. doi:10.1088/1741-4326/aa6489.

[3] J. L. Hou *et al.*, "Dependence of upstream SOL density shoulder on divertor neutral pressure in EAST," *Nucl. Fusion*, vol. 61, 076018, 2021. doi:10.1088/1741-4326/ac01f4.

[4] D. Carralero *et al.*, "Experimental validation of a filament transport model in turbulent magnetised plasmas," *Phys. Rev. Lett.*, vol. 115, 215002, 2015. doi:10.1103/PhysRevLett.115.215002.

[5] A. Kirk *et al.*, "A comparison of H-mode pedestal characteristics in MAST as a function of magnetic configuration and ELM type," *Plasma Phys. Control. Fusion*, vol. 51, 065016, 2009. doi:10.1088/0741-3335/51/6/065016.

[6] J. R. Harrison *et al.*, "Benefits of the Super-X divertor configuration for scenario integration on MAST Upgrade," *Plasma Phys. Control. Fusion*, vol. 66, 065019, 2024. doi:10.1088/1361-6587/ad4058.

[7] S. Mordijck *et al.*, "Impact of ionization and transport on pedestal density structure in DIII-D and Alcator C-Mod," *Nucl. Fusion*, vol. 64, 126034, 2024. doi:10.1088/1741-4326/ad52ca.

[8] S. Mordijck, "Overview of density pedestal structure: role of fueling versus transport," *Nucl. Fusion*, vol. 60, 082006, 2020. doi:10.1088/1741-4326/ab8d25.